Polynomial Feedforward Design Techniques for a Mechanical Wave Diode System*

Peter Nauclér† Torsten Söderström†

Abstract

This paper considers feedforward control of extensional waves in a bar. The system is designed to have properties analogous to those of an electrical diode and is therefore referred to as a *mechanical wave diode*. We present three different feedforward control strategies. Two of them relies on an 'ideal' design which is derived in the noise-free case, whereas the third is based on Wiener filtering theory.

The control strategies are compared and evaluated for different signal models and in the presence of measurement noise. We show that the performance of the device is improved by using the (optimal) Wiener feedforward filter.

1 Introduction

Many mechanical structures consist of slender beam elements that can be considered to act as wave guides. In such structures, waves may propagate from a disturbance source along the structure as extensional, torsional and flexural waves [8, 5]. Traditionally, passive techniques have been used to reduce mechanical waves and vibrations. Sometimes, however, such solutions are less suitable. This can be the case in *e.g.* applications where the weight of the structure is a limiting factor.

*Research partially supported by the Swedish Research Council, contract 621-2001-2156

†Department of Information Technology, Uppsala University. P.O. Box 337, SE-751 05 Uppsala, Sweden. Email: {Peter.Naucler, Torsten.Soderstrom}@it.uu.s

Active structures have been the topic of intense research the last decades. These structures have the ability to actuate the system with secondary inputs in order to obtain some desired structural response. This is performed by incorporating sensors and actuators into the structure [3, 11, 13].

This paper is concerned with the design of feedforward control strategies for extensional waves in a bar. The system is designed to fully reflect waves traveling in one direction and fully transmit waves from the other direction. Therefore, it has similar properties to those of an electrical diode and is referred to as a 'mechanical wave diode'. The concept of such a device was originally introduced in [12]. Here, we extend those results with more general control strategies.

1.1 Notation

The following notational conventions are used in this paper.

T	sampling period
τ	time delay (in samples)
q^{-1}	backward shift operator, $q^{-1}y(t) = y(t-T)$
nP	degree of polynomial P
$P = P(q^{-1})$	$p_0 + p_1 q^{-1} + \cdots + p_{nP} q^{-nP}$
P^*	$p_0^* + p_1^* q \quad + \cdots + p_{nP}^* q^{nP}$ (reciprocal polynomial)
x	scalar
$\mathbf{x}$	vector
$\mathbf{X}$	matrix

When appropriate, the complex variable z is substituted for the forward shift operator q. The polynomial arguments q^{-1}, z^{-1} are sometimes omitted in order to simplify the notation. The zeros of the polynomial $P(z^{-1})$ are the solutions to $z^{nP}P(z^{-1}) = 0$.

2 Modeling

Consider propagation of elastic waves in a straight bar as shown in Figure 1. At two sections, the bar is equipped with strain gauge pairs. Also, along a segment of the bar, a pair of piezo-electric actuators, electrically and mechanically in parallel, are attached. The idea with this configuration of bar, sensors and actuator is to apply feedforward control so that waves traveling from the sensors towards the first bar-actuator interface will be

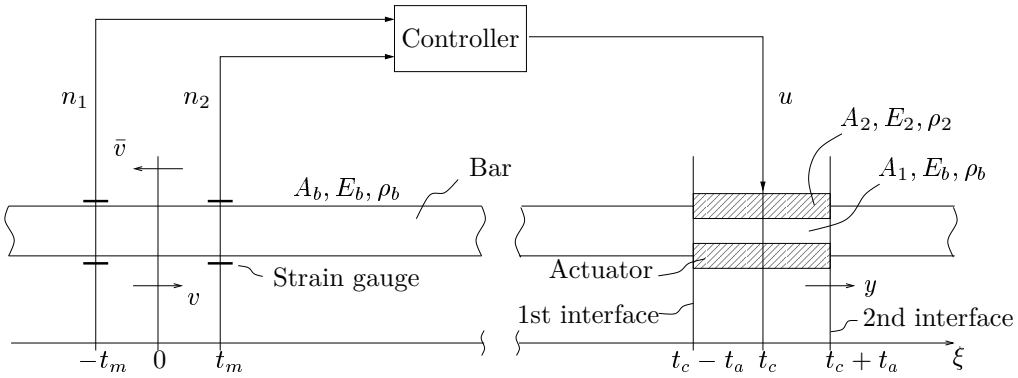

Figure 1: Bar with two strain gauge pairs, one actuator pair and feedforward control for one-way transmission from left to right.

fully reflected while waves traveling in the opposite direction, towards the second bar/specimen interface, will be transmitted undisturbed. Therefore, waves traveling from the sensors towards the first bar/actuator interface will be considered measurable disturbances which are to be suppressed through feedforward control.

2.1 Electromechanical Modeling

In Figure 1, A, E and ρ denote cross-sectional area, Young's modulus and density, respectively. These quantities differ for different sections of the bar. For given properties of the bar and actuator materials, the cross-sectional areas A_1 and A_2 are assumed to be chosen so that impedance matching is achieved. Therefore, the waves $\bar{v}$ and v traveling back and forth in the structure are transmitted undisturbed through the actuator region if no control action is applied. The wave motion in the bar can be expressed in terms of the Fourier transform of the normal force as

$$N(\xi, \omega) = V(\omega)\mathrm{e}^{-\mathrm{i}\omega\xi} + \bar{V}(\omega)\mathrm{e}^{-\mathrm{i}\omega\xi} \tag{1}$$

where ξ is a transformed axial coordinate with dimension of time [12], $V(\omega)$ and $\bar{V}(\omega)$ are the Fourier transforms of $v(t)$ and $\bar{v}(t)$, respectively. In the time domain, (1) means that waves propagates through the bar without damping and that superposition holds.

In [12], we extensively describe the electromechanical modeling of the wave diode system. Here, we will briefly review the final modeling in discrete time, where it is assumed that the time delays t_a, t_m and t_c are integer

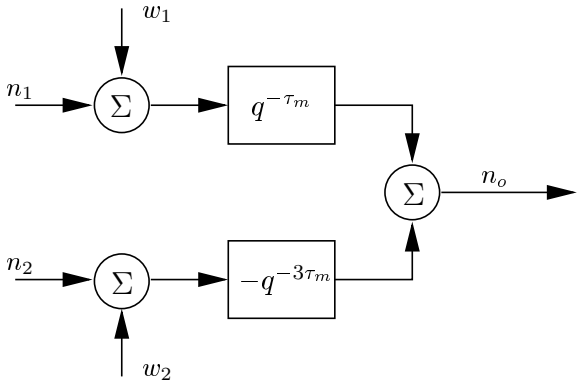

Figure 2: Decoupling setup.

multiples of of the sampling interval T. We label these multiples as τ_a, τ_m and τ_c, respectively, so that $t_a = \tau_a T$, *etc.* This means that we can use the backward shift operator q^{-1} so that, e.g., $q^{-\tau_a} n(t) = n(t - \tau_a T) = n(t - t_a)$.

Generally, the waves represented by v and $\bar{v}$ overlap in the time domain. Therefore, the disturbance v cannot be measured directly. However, the waves traveling back and forth in the bar can be separated if n_1 and n_2 are measured strains at two different bar sections $\xi_1 = -t_m$ and $\xi_2 = t_m$ as in Figure 1 [10]. The measurements are then filtered in a way that is depicted in Figure 2. The filtering can be viewed as a decoupling since it removes the $\bar{v}$ component that is carried by n_1 and n_2. The fact that $\bar{v}$ is indeed filtered out can be seen by equating the filter equations for n_o,

$$\begin{aligned} n_o(t) &= q^{-\tau_m}[n_1(t) + w_1(t)] - q^{-3\tau_m}[n_2(t) + w_2(t)] \\ &= q^{-\tau_m}[q^{\tau_m} v(t) + q^{-\tau_m}\bar{v}(t) + w_1(t)] \\ &\quad - q^{-3\tau_m}[q^{-\tau_m} v(t) + q^{\tau_m}\bar{v}(t) + w_2(t)] \\ &= B_1(q^{-1})v(t) + w(t) \end{aligned} \tag{2}$$

with

$$\begin{aligned} B_1 &= 1 - q^{-4\tau_m} \\ w(t) &= q^{-\tau_m} w_1(t) - q^{-3\tau_m} w_2(t). \end{aligned}$$

Here, $w(t)$ is the assembled effect of the two noise sources. The second equality in (2) follows from the wave equation (1) and how n_1 and n_2 are defined in Figure 1. In the sequel, n_o is treated as a 'virtual' measured signal that only depends on v and w, and not on $\bar{v}$. This signal is used as input signal to the feedforward controller. The output from the controller $u(t)$ is fed to the actuator. It has the input-output relation

$$y^{(c)}(t) = B_2(q^{-1})u(t)$$

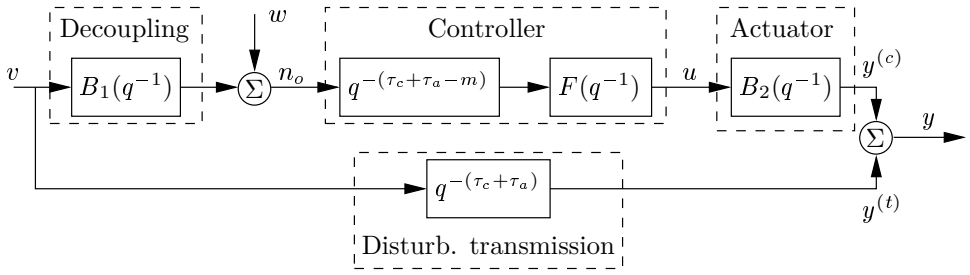

Figure 3: Schematic view of the wave diode system.

where

$$B_2(q^{-1}) = \frac{1}{2}\left(1 - q^{-2\tau_a}\right),$$

which is derived in [7] and modified to discrete time in [12]. The signal $y^{(c)}$ denotes the part of the output signal y that is deduced from the control action. The part of the output that originates from the disturbance transmission in the bar, $y^{(t)}(t)$, is a pure time delay of v,

$$y^{(t)}(t) = q^{-(\tau_c+\tau_a)}v(t), \tag{3}$$

according to (1) and the bar configuration in Figure 1, where $y(t) = y^{(c)}(t) + y^{(t)}(t)$ is defined at the 2nd interface. Finally, we model the time delay that occurs in the feedforward link due to hardware limitations *etc.* In order to prevent a need for signal prediction in the feedforward filter, this time delay is not allowed to be larger than the disturbance transmission delay, which is $(\tau_c + \tau_a)T$, see (3). Therefore, these time delays are put in relation and the control loop delay is modeled as $(\tau_c + \tau_a - m)T$, with $m \geq 0$. Thus, the delay in the feedforward filter is m samples *less* than the delay due to disturbance transmission.

By use of the relations introduced so far the system can be schematically realized as shown in Figure 3, with the single input $v(t)$ and single noise source $w(t)$. The measured signals n_1 and n_2 are 'hidden' in n_o as described by (2). The expressions for the output signal and control signal as functions of the disturbance and measurement noise can then be written as

$$y(t) = \left[1 + q^m B_2 F B_1\right] q^{-(\tau_c+\tau_a)}v(t) + B_2 F q^{-(\tau_c+\tau_a-m)}w(t) \tag{4}$$

$$u(t) = q^m F B_1 q^{-(\tau_c+\tau_a)}v(t) + F q^{-(\tau_c+\tau_a-m)}w(t). \tag{5}$$

The following values of the system parameters are chosen for illustrations and numerical examples:

$$T = 5\,\mu s$$
$$\{\tau_a, \tau_m, \tau_c\} = \{2, 8, 200\}.$$

These values coincide with the ones employed in [12].

2.2 Signal Modeling

The disturbance $v(t)$ and the measurement noise $w(t)$ are modeled as ARMA processes,

$$v(t) = \frac{C(q^{-1})}{D(q^{-1})}\tilde{v}(t) \quad w(t) = \frac{M(q^{-1})}{N(q^{-1})}\tilde{w}(t)$$

with driving noise variances $\lambda^2_{\tilde{v}}$ and $\lambda^2_{\tilde{w}}$, respectively. It is assumed that $v(t)$ and $w(t)$ are mutually independent.

These models are quite general. One can employ ARMA models for modeling of stochastic signals as well as deterministic-like signals, such as steps, pulses *etc.* as discussed in [9, 12]. In this paper we will treat two cases for numerical examples,

Case (i)		**Case (ii)**	
$C = 1$	$M = 1$	$C = 0.1$	$M = 0.5$
$D = 1$	$N = 1$	$D = 1 - 0.9q^{-1}$	$N = 1 - 0.5q^{-1}$.

The first case treats white disturbance and measurement noise, whereas the second case treats a disturbance of low frequency content and a noise source with broader spectrum.

2.3 Ideal Feedforward Controller

The ideal feedforward filter, as derived in [12] is

$$F(q^{-1}) = -\frac{q^{-m}}{B_1 B_2} = \frac{-2q^{-m}}{(1 - q^{-4\tau_m})\,(1 - q^{-2\tau_a})}, \tag{6}$$

which performs perfectly in the noise-free case, yielding $y(t) = 0$. However, if measurement noise is present the output variance will grow linearly with time. This is due to the poles of (6) lying on the unit circle, and the measurement noise will contribute to the output as a random walk process after passing (6). Therefore, the ideal design needs to modified to be useful in a realistic scenario where measurement noise is present.

3 Feedforward Design

In this section three different ways of designing asymptotically stable feedforward filters are presented. The first two techniques utilize the structure of the ideal design and are therefore referred to as 'fixed feedforward structures'. The third feedforward design is instead based Wiener filtering techniques.

The first approach was originally introduced and analyzed in [12], whereas the other two are novel for this paper.

3.1 Fixed Feedforward Structures

The two fixed feedforward approaches are both based on modifying the ideal design (6) by moving its poles towards the origin to make the filter asymptotically stable. The modification is

$$F(q^{-1}) = \frac{-2q^{-m}}{(1 - r_1 q^{-4\tau_m})\,(1 - r_2 q^{-2\tau_a})},$$

where r_1 and r_2 are real numbers in the interval [0, 1). These parameters are design variables that can be adjusted to minimize some cost function. The criteria we utilize are based on computing the variances of $y(t)$ and $u(t)$. In order to perform this it is useful to first realize the system in state-space form. Such a realization has the structure

$$\begin{aligned} \mathbf{x}(t+T) &= \mathbf{\Phi}(r_1, r_2)\mathbf{x}(t) + \mathbf{\Gamma} \begin{bmatrix} \tilde{v}(t) \\ \tilde{w}(t) \end{bmatrix} \\ \begin{bmatrix} y(t) \\ u(t) \end{bmatrix} &= \mathbf{H}\mathbf{x}(t) \end{aligned} \tag{7}$$

where the dependence of r_1, r_2 on Φ is stressed. The state-space realization can be obtained using *e.g.* some kind of canonical form [4]. Of course, (7) will also depend on the signal models for $v(t)$ and $w(t)$.

Then, the output variance and the control signal variance can be computed as [14]

$$E \begin{bmatrix} y^2(t) & * \\ * & u^2(t) \end{bmatrix} = \mathbf{H}\mathbf{P}\mathbf{H}^{\mathbf{T}}$$

where $*$ denotes a (non-interesting) cross term and $\mathbf{P}$ is the covariance matrix of the state vector $\mathbf{x}$, which is computed by solving the Lyapunov equation

$$\mathbf{P} = \mathbf{\Phi}\mathbf{P}\mathbf{\Phi}^{\mathbf{T}} + \mathbf{\Gamma} \begin{bmatrix} E\tilde{v}^2(t) & 0 \\ 0 & E\tilde{w}^2(t) \end{bmatrix} \mathbf{\Gamma}^T. \tag{8}$$

In (8) the assumption that $v(t)$ and $w(t)$ are mutually independent is utilized. This procedure of variance computation will also be useful in Section 4, where the different control strategies are evaluated.

3.2 Fixed one-DOF Design

In the first approach for feedforward design, all poles of the feedforward filter are constrained to be placed at the same distance to the origin. This is achieved by minimization of the criterion

$$J_1 = Ey^2(t) \quad \text{s.t. } r_2 = r_1^{\tau_a/2\tau_m}. \tag{9}$$

Due to the coupling between r_1 and r_2 this filter has only one degree of freedom (DOF) and is therefore referred to as a fixed one-DOF structure. The constraint to place all poles on the same circle is one way to make the feedforward filter *asymptotically* stable. If r_1 and r_2 are treated as independent design variables it turns out that $Ey^2(t)$ will decrease as r_2 approaches 1. However, the output variance is not defined for $r_2 = 1$, since this would cancel common poles and zeros on the unit circle, *c.f.* (4). In addition, $r_2 = 1$ would cause $u(t)$ to be a random walk process with a variance that grows unbounded.

The minimum point of (9) is found in a numerical search procedure. The equation (8) is repeatedly solved for different values of r_1 and r_2. Due to the coupling between the two parameters the optimization is carried out in one dimension.

In Figure 4(a) the result of such a procedure is shown for case (i). For purpose of illustration the output signal is decomposed in a signal part and a noise part, *i.e.*

$$y(t) = y_v(t) + y_w(t),$$

and their respective variances as functions of r_1 are shown in the figure. It portrays the tradeoff between disturbance rejection and measurement noise sensitivity. The variance of the signal part decreases as r_1 approaches 1, while at the same time the variance of the noise part rapidly increases. In the example, the SNR is set to 20 dB and the minimum value of the cost function is obtained for $r_1 = 0.9141$ and $r_2 = 0.9888$.

3.3 Fixed two-DOF Design

Another way to guarantee the feedforward filter to be asymptotically stable is to penalize the control signal in the criterion to minimize. Such a cost function is

$$J_2 = Ey^2(t) + \rho Eu^2(t),$$

where $\rho > 0$. The amount of penalty on the control signal determines how close r_2 should be to 1. A small value of ρ gives $2\tau_a$ number of poles close to the unit circle and vice versa. The optimization procedure is carried out in a similar fashion as for the one-DOF structure. The difference is that also $Eu^2(t)$ is employed for each new set of $\{r_1,\, r_2\}$ and that the optimization is carried out in two dimensions, since the parameters are treated as independent design variables. Therefore, the obtained feedforward filter is referred to as a fixed two-DOF structure.

For case (i), a contour plot of the cost function is shown in Figure 4(b). Here, $\rho = 10^{-3}$ and SNR = 20 dB are chosen. The value of the cost function for different level curves are shown in the plot and the minimum point is obtained for $r_1 = 0.9038$ and $r_2 = 0.9408$.

For both of the two fix feedforward structures the optimum values of r_1 and r_2 will depend on the SNR. For high noise levels, their values will decrease to diminish the effect of the noise and vice versa.

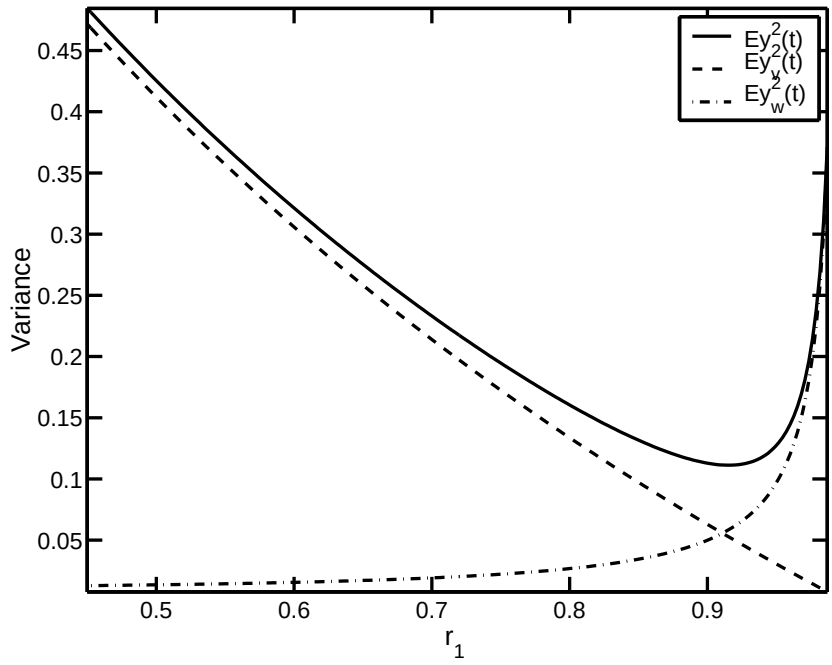

(a) One-DOF feedforward

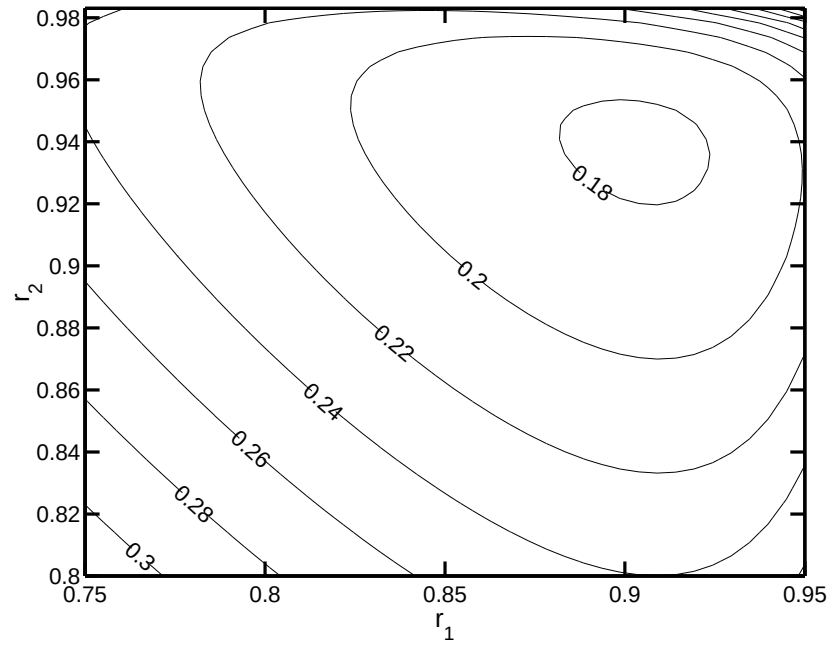

(b) Two-DOF feedforward

Figure 4: Case (i). (a) Output variance as a function of r_1 and (b) cost function J_2 in a contour plot as a function of r_1 and r_2. SNR = 20 dB.

3.4 Design based on Wiener Filter Theory

The Wiener filter procedure is different from the other two design principles in the sense that no prior feedforward structure is utilized. The Wiener filter is designed to optimally minimize the cost function

$$J_3 = Ey^2(t|t+m) + \rho Eu^2(t|t+m),$$

where $m \geq 0$ is used as a fixed lag smoothing parameter to possibly improve the performance of the feedforward filter.

Wiener filters are usually designed to recover some desired signal from noisy measurements. The classical approach to realize such a filter is to utilize the statistical relation between the desired signal and the measured signal by employing the Wiener-Hopf equations [6]. Other methods include variational arguments and the completing the squares approach [2]. For the wave diode system, the difficulty is that it is not possible to pose a Wiener problem in a usual way. One cannot find two correlating signals that can be used to produce an asymptotically stable feedforward filter.

Instead, the cost function is evaluated using frequency domain relations and we notice that the obtained structure can be utilized to produce a Wiener solution for the feedforward filter. Expressing the output variance and control signal variance by use of Parseval's relation yields

$$\begin{aligned} Ey^2(t|t+m) &= \frac{1}{2\pi \mathrm{i}} \oint_{|z|=1} \left(1 + z^m B_2 F B_1\right) \left(1 + z^m B_2 F B_1\right)^* \Phi_v \frac{\mathrm{d}z}{z} \\ &\quad + \frac{1}{2\pi \mathrm{i}} \oint_{|z|=1} B_2 B_2^* F F^* \Phi_w \frac{\mathrm{d}z}{z} \\ Eu^2(t|t+m) &= \frac{1}{2\pi \mathrm{i}} \oint_{|z|=1} F F^* B_1 B_1^* \Phi_v \frac{\mathrm{d}z}{z} + \frac{1}{2\pi \mathrm{i}} \oint_{|z|=1} F F^* \Phi_w \frac{\mathrm{d}z}{z} \end{aligned}$$

and the cost function is readily evaluated,

$$\begin{aligned} J_3 &= \frac{1}{2\pi \mathrm{i}} \oint_{|z|=1} \big(\Phi_v + F z^m B_2 B_1 \Phi_v + B_1^* B_2^* z^{-m} \Phi_v F^* \\ &\quad + F \left[B_2 B_2^* B_1 B_1^* \Phi_v + B_2 B_2^* \Phi_w + \rho \left(B_1 B_1^* \Phi_v + \Phi_w \right) \right] F^* \big) \frac{\mathrm{d}z}{z} \\ &\triangleq \frac{1}{2\pi \mathrm{i}} \oint_{|z|=1} \left(\Phi_v - F \Phi_{zv} - \Phi_{vz} F^* + F \Phi_z F^* \right) \frac{\mathrm{d}z}{z}. \end{aligned} \tag{10}$$

In (10), the spectra Φ_z and Φ_{sz} are defined as

$$\begin{aligned}\Phi_z &= B_2B_2^*B_1B_1^*\Phi_v + B_2B_2^*\Phi_w + \rho\left(B_1B_1^*\Phi_v + \Phi_w\right)\\ &= \left(B_1B_1^*\Phi_v + \Phi_w\right)\left(B_2B_2^* + \rho\right) \qquad (11)\\ \Phi_{vz} &= -B_1^*B_2^*z^{-m}\Phi_v \qquad (12)\end{aligned}$$

The signal $z(t)$ has no physical interpretation that could be shown in *e.g.* Figure 3. It is rather an instrument in formulating the Wiener solution for minimization of the cost function J_3. The structure in (10) appears when formulating the Wiener problem by using the *completing the squares approach* [2]. The 'direct' Wiener solution,

$$F(z^{-1}) = \Phi_{vz}(z^{-1})\Phi_z^{-1}(z^{-1}),$$

is generally unrealizable since it is non-causal. The realizable Wiener filter is instead obtained by first computing an innovations representation of $z(t)$ and then extracting the causal part ($[\ ]_+$) of a filter [14].

The innovations representation can be written as

$$z(t) = H(q^{-1})\varepsilon(t),$$

where the innovations sequence ε is white with variance λ_ε^2 is determined by use of spectral factorization. The filter H is minimum phase and asymptotically stable. Inserting the expressions for the spectra of $v(t)$ and $w(t)$ in (11) yields

$$\left(\frac{B_1B_1^*CC^*}{DD^*}\lambda_v^2 + \frac{MM^*}{NN^*}\lambda_w^2\right)\left(B_2B_2^* + \rho\right) = HH^*\lambda_\varepsilon^2, \qquad (13)$$

where

$$H = \frac{\beta}{DN}.$$

The structure of H is determined by setting the left hand side of (13) on common denominator form. The polynomial β can be computed by two spectral factorizations; one for each factor of (13),

$$B_1B_1^*CC^*NN^*\lambda_v^2 + MM^*DD^*\lambda_w^2 = \beta_1\beta_1^*\lambda_{\varepsilon_1}^2 \qquad (14)$$

$$B_2B_2^* + \rho = \beta_2\beta_2^*\lambda_{\varepsilon_2}^2, \qquad (15)$$

where $\beta = \beta_1\beta_2$ and $\lambda_\varepsilon^2 = \lambda_{\varepsilon_1}^2\lambda_{\varepsilon_2}^2$. Then, the filter that minimizes J_3 is [14],[2]

$$\begin{aligned}F(z^{-1}) &= \left[\Phi_{vz}\left\{H^*\right\}^{-1}\frac{1}{\lambda_\varepsilon^2}\right]_+ H^{-1}\\ &= \frac{\lambda_v^2}{\lambda_\varepsilon^2}\left[\frac{B_1^*B_2^*z^{-m}CC^*N^*}{D\beta^*}\right]_+\frac{DN}{\beta}. \qquad (16)\end{aligned}$$

The causal bracket $[\ ]_+$ in (16) can be evaluated by solving a Diophantine equation [2]. This can be seen by writing the expression as a sum of a causal and strictly anti-casual part,

$$\left[\frac{B_1^* B_2^* z^{-m} C C^* N^*}{D\beta^*}\right]_+ = \left[\frac{Q}{D}\right]_+ + \underbrace{\left[z\frac{L^*}{\beta^*}\right]_+}_{=0}, \tag{17}$$

where Q and L^* are polynomials in z^{-1} and z, respectively, of degree

$$\begin{aligned} nQ &= \max\{nC + m, nD - 1\} \\ nL &= \max\{nB_1 + nB_2 + nC + nN - m, n\beta\} - 1. \end{aligned}$$

The Diophantine equation is obtained by expressing the right hand side of (17) on common denominator form (ignoring the brackets),

$$B_1^* B_2^* z^{-m} C C^* N^* = \beta^* Q + z D L^*, \tag{18}$$

and the optimal filter is obtained using (16) and (17),

$$F(z^{-1}) = \frac{\lambda_v^2}{\lambda_\varepsilon^2}\frac{Q(z^{-1})N(z^{-1})}{\beta(z^{-1})}. \tag{19}$$

The Diophantine equation (18) will have a unique solution due to the construction of Q and L^*, as described in [1].

A remark regarding the choice of ρ: It can be seen from (15) that $\rho = 0$ generates a feedforward filter with poles on the unit circle. This is due to the fact that β then would have a factor B_2, which leads to a feedforward filter that is only marginally stable when (19) is computed. Thus, $\rho = 0$ is not a permitted choice.

Before turning to the numerical examples where the different feedforward design approaches are compared it can be of interest to evaluate the effect of smoothing for the Wiener filter. In Figure 5, $Ey^2(t)/Ev^2(t)$ is shown as a function of the smoothing parameter m. The y-axis then show how much is gained by employing feedforward control. The SNR, $Ev^2(t)/Ew^2(t)$ is tuned to 5 dB. It can be seen that for both cases the output variance decreases almost stepwise for integer multiples of $4\tau_m = 32$.

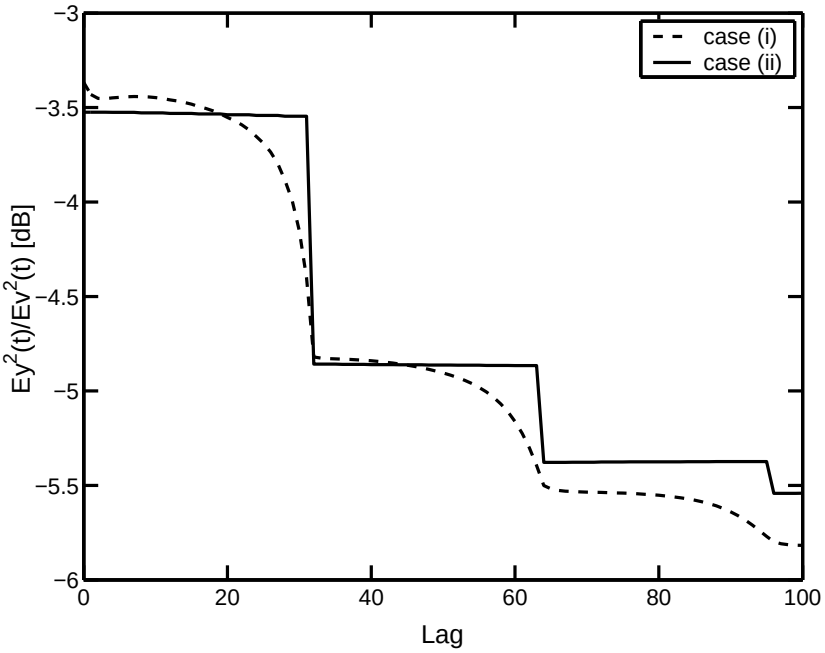

Figure 5: The effect of smoothing for SNR = 5 dB and $\rho = 10^{-3}$.

4 Numerical Examples

In this section the different feedforward control strategies are evaluated and compared for different SNR values. The one-DOF, two-DOF and Wiener feedforward filters are denoted F_1, F_2 and F_3, respectively. For F_2 and F_3, $\rho = 10^{-3}$ is chosen. The Wiener feedforward filter is evaluated for pure filtering ($m = 0$) and smoothing with $m = 32$. For the latter, not much is gained by choosing a smaller value of m and larger values may give unnecessarily long time delay constraints to make the controller causal.

The output variance and the cost function with control signal penalty are employed as performance measures. These quantities are normalized with the variance of the disturbance, $Ev^2(t)$.

The results for cases (i) and (ii) are reported in Figure 6 and Figure 7, respectively. The (a)-parts of the figures show the output variance as a function of the SNR in dB scales. The interpretation should be that the feedforward control is efficient for SNR values that yield outputs below 0 dB. If the output quantity reaches above 0 dB, the control loop amplifies the disturbance $v(t)$ and the wave diode becomes useless.

The (b)-parts of the figures depict the cost function measure $[Ey^2(t) + \rho Eu^2(t)]/Ev^2(t)$. Here, the Wiener filter F_3 should give better performance than F_1 and F_2. This is due to the fact that it in some sense has the 'truly optimal' structure.

Both cases demonstrate similar results for the different design techniques. The two feedforward filters based on Wiener filtering yield the best performance in terms of cost function evaluation. The Wiener filter with fixed lag smoothing gives the lowest value since this filter utilizes 'future' data.

In terms of output variance minimization, the Wiener filters also give the best overall performance. For high SNR values the one-DOF feedforward filter F_1 gives very low output variance. It may even beat the Wiener filter structures. This is to the expense of a very high control signal variance. Notice that F_1 is not designed to take the magnitude of the control signal into account. The effect of this can be seen in Figures 6, 7 (b) where the variance of the control signal dominates for high signal to noise ratios. Here, F_1 clearly gives a substantial performance degradation compared to the other design techniques.

The overall performance of the two-DOF filter F_2 lies somewhat in-between F_1 and F_3. It performs similar to F_1 for low to moderate SNR values.

However, it lacks F_1:s drawback of a substantial control signal variance for high SNR.

An observation is that F_1 and F_2 performs relatively better for case (i) than for case (ii). This is natural since the structures of these two feedforward filters do not take noise dynamics into account, which is present in the second case.

Another issue is robustness against modeling errors. In Figure 8, the case of inaccurate signal models are evaluated. The system is here operating with the signal models of case (ii), whereas the feedforward design is carried out under the assumption of case (i). Therefore, Figure 8 should be compared to Figure 7 since both figures reports results from identical systems. It can be seen that the performance of the feedforward filter is only slightly degraded when wrong signal models are utilized and that the different design strategies keep their joint grading. A circumstance that perhaps can be seen a bit ambiguous is that the cost function measure for F_1 actually is a bit improved in Figure 8 compared to Figure 7. The explanation is that the control signal is not accounted for in the design of F_1, see (9).

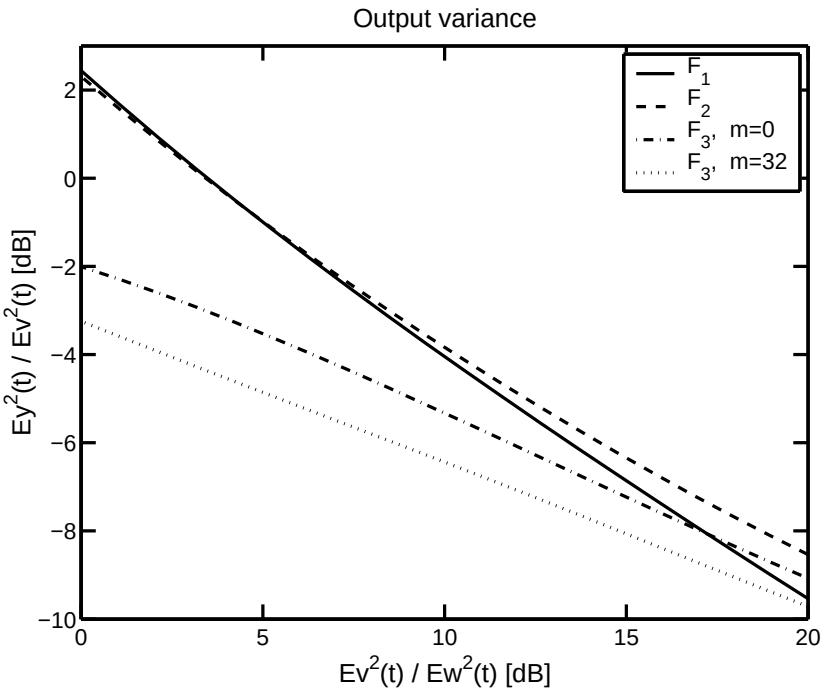

(a)

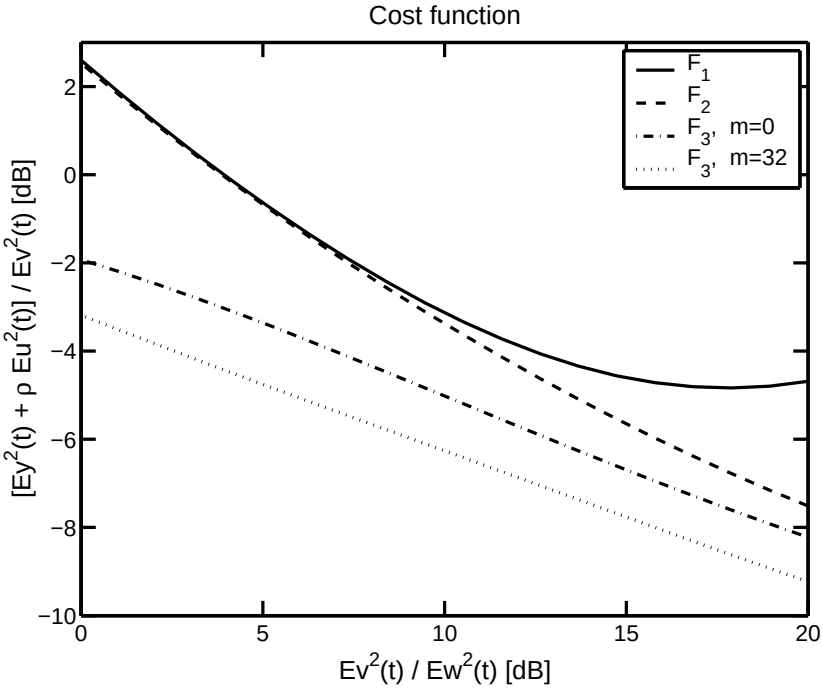

(b)

Figure 6: Case (i). Evaluation of (a) the output variance and (b) the cost function with control signal penalty.

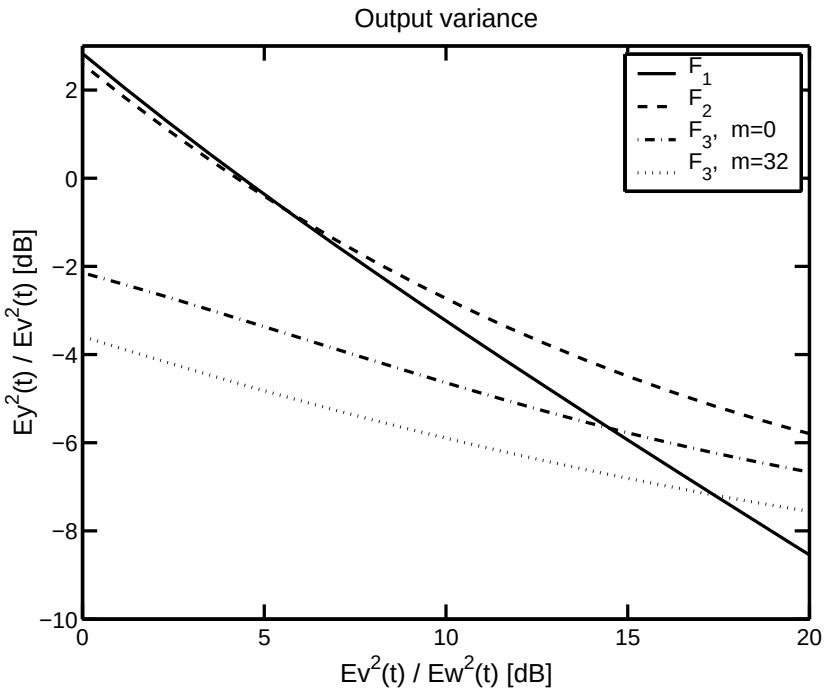

(a)

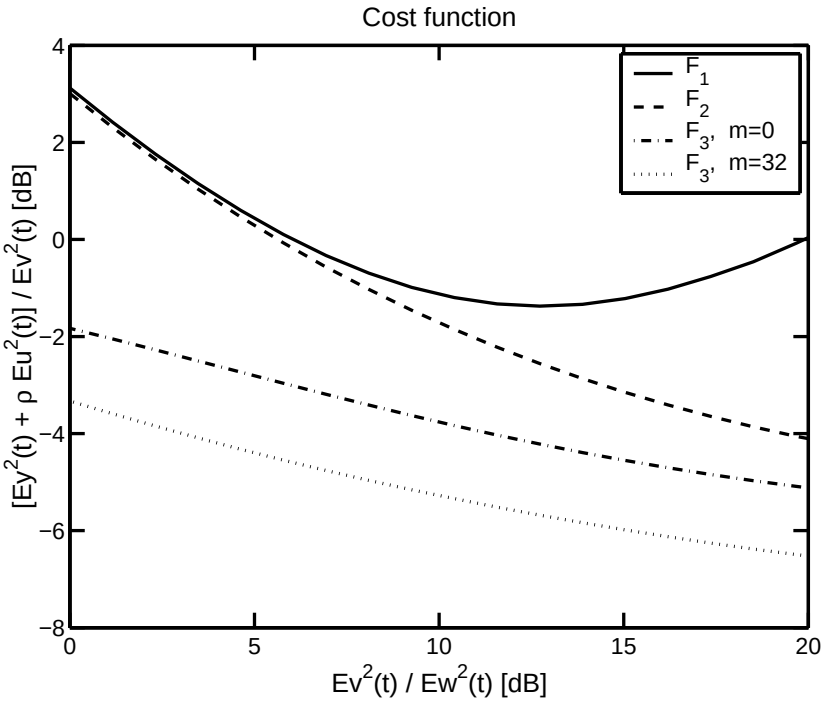

(b)

Figure 7: Case (ii). Evaluation of (a) the output variance and (b) the cost function with control signal penalty.

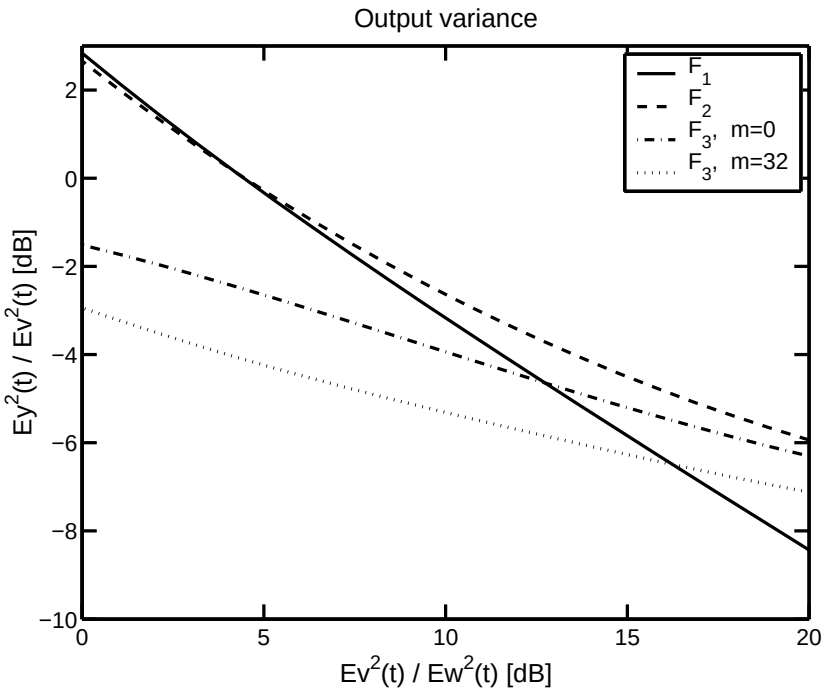

(a)

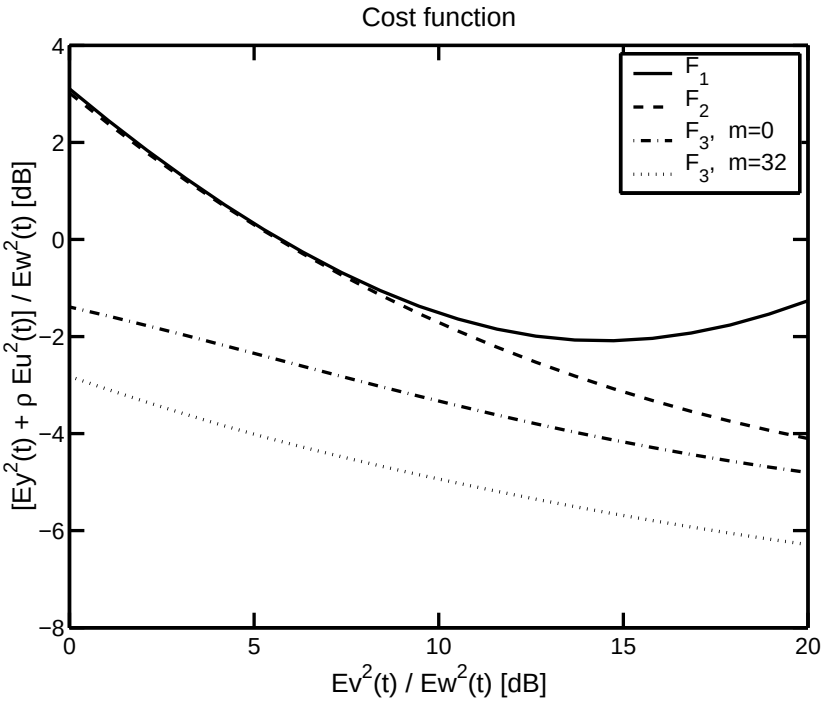

(b)

Figure 8: Robustness examination. Design based on case (i), whereas the true system applies to case (ii).

5 Conclusions

In this paper, the results reported in [12] are extended with more general types of feedforward control strategies. An apparent motivation for the work is to investigate how much can be gained by utilizing an optimal design strategy that does not presume a pre-determined model structure. In order to accomplish this, a criterion with control signal penalty is introduced, which allows optimal feedforward control design with Wiener filtering techniques. This is in contrast to the previous work that only considered output variance minimization with constraint on the pole locations for a pre-determined feedforward structure.

Numerical examples show that by use of Wiener filtering, the overall performance (including both output variance and control signal variance) can be improved over a wide range of signal to noise ratios. Due to the transmission delay of disturbing waves traveling in the bar, one may also apply fixed lag smoothing in the feedforward link to further improve the performance.

The amount of smoothing that one can allow is set by physical limitations. For the controller to be casual the transmission delay cannot be shorter than the sum of mT and the control loop delay. Therefore, a large value of m may lead to a very long mechanical structure in order to increase the wave transmission delay.

The two 'fixed' feedforward structures are optimized over only one and two parameters, respectively. However, the structures of these feedforward filters are chosen with prior knowledge of the 'ideal' feedforward filter (6). The numerical examples show that these two design strategies perform quite well. Especially for high SNR values they may challenge the Wiener structure in terms of output variance minimization.

Despite its theoretical elaborateness, the Wiener structure has the lowest computational complexity in the design phase. This is due to the fact that the two 'fixed' feedforward structures are computed by means of a numerical search procedure, where a Lyapunov equation is solved in each step. In terms of implementation, the Wiener structure is generally of highest complexity. The order of F_1 and F_2 are both $nB_1 + nB_2$, whereas F_3 is of order $\max\{nB_1 + nC + nN, nD + nM\} + nB_2$. The difference is, however, of minor importance.

Regarding optimality, one should remember that the Wiener feedforward type of controller is only optimal under the assumption that the models do describe the system. However, when the design is based on false sig-

nal models, all feedforward filters still perform similarly as before. Their performances are only slightly degraded.

The evaluation of the optimal feedforward filter shows how much can be gained by choosing a 'complex' feedforward structure instead of the simpler one, that was derived from the 'ideal' controller (6). The conclusion is that it actually is worthwhile to employ the Wiener filter structure. The main achievement is that the output variance can be kept low for a wide range of SNR values and at the same time keeping the control signal variance at moderate levels.

References

[1] A. Ahlén and M. Sternad. Optimal deconvolution based on polynomial methods. *IEEE Trans. on Acoustics Speech and Signal Processing*, 37:217–226, 1989.

[2] A. Ahlén and M. Sternad. Derivation and design of Wiener filters using polynomial equations. In C.T. Leondes, editor, *Control and Dynamic Systems, Vol 64: Stochastic Techniques in Digital Signal Processing Systems*, pages 353–418, USA, 1994. Academic Press.

[3] C. R. Fuller, S. J. Elliott, and P. A. Nelson. *Active Control of Vibration*. Academic Press, London, 1996.

[4] T. Glad and L. Ljung. *Control Theory*. Taylor and Francis, UK, 2000.

[5] K. G. Graff. *Wave Motion in Elastic Solids*. Clarendon Press, Oxford, UK, 1975.

[6] M.H. Hayes. *Statistical Signal Processing and Modeling*. J. Wiley & Sons, Inc, USA, 1996.

[7] A. Jansson and B. Lundberg. Piezoelectric generation of extensional waves in a viscoelastic bar by use of a linear power amplifier: Theoretical basis. *Journal of Sound and Vibration*, 306:318–332, 2007.

[8] H. Kolsky. *Stress Waves in Solids*. Dover Publications, Inc, New York, 1963.

[9] L. Ljung. *System Identification*. Prentice–Hall, Upper Saddle River, NJ, USA, 2nd edition, 1999.

[10] B. Lundberg and A. Henchoz. Analysis of elastic waves from two-point strain measurement. *Experimental Mechanics*, 17:213–218, 1977.

[11] S. O. R. Moheimani, D. Halim, and A. J. Fleming. *Spatial Control of Vibration: Theory and Experiments*. World Scientific Publishing Co. Pte. Ltd., Singapore, 2003.

[12] P. Nauclér, B. Lundberg, and T. Söderström. A mechanical wave diode: Using feedforward control for one-way transmission of elastic extensional waves. *IEEE Trans. on Control Systems Technology*, 15(4):715–724, 2007.

[13] A. Preumont. *Vibration Control of Active Structures: An Introduction*. Kluwer Academic Publisher, Dordrecht, 2002.

[14] T. Söderström. *Discrete-time Stochastic Systems*. Springer-Verlag, London, UK, 2nd edition, 2002.